Mathematics

https://www.aimspress.com/journal/Math

AIMS Mathematics, 9(11): 30816–30837.
DOI:10.3934/math.20241488
Received: 11 September 2024
Revised: 16 October 2024
Accepted: 22 October 2024
Published: 30 October 2024

Research article

Pattern formation of a volume-filling chemotaxis model with a bistable source

Zuojun Ma[1,2,*]

[1] School of Mathematics and Information Engineering, Longdong University, Qingyang 745000, China

[2] Institute of Applied Mathematics, Longdong University, Qingyang 745000, China

* **Correspondence:** Email: mzjun8906@163.com.

Abstract: In this paper, the pattern formation of a volume-filling chemotaxis model with bistable source terms was studied. First, it was shown that self-diffusion does not induce Turing patterns, but chemotaxis-driven instability occurs. Then, the asymptotic behavior of the chemotaxis model was analyzed by weakly nonlinear analysis with the method of multiple scales. When the chemotaxis coefficient exceeded a threshold value and there was a single unstable mode, the supercritical and subcritical bifurcation of the model was discussed. The amplitude equations and the asymptotic expressions of the patterns were obtained. When the chemotaxis coefficient was large enough, the two-mode competition behavior of the model with two unstable modes was analyzed, and the corresponding amplitude equations and the asymptotic expressions of the patterns were obtained. Finally, numerical simulations were provided to further illuminate the above analytical results.

Keywords: chemotaxis; volume-filling; bistable; pattern formation; weakly nonlinear analysis; amplitude equation
Mathematics Subject Classification: 35K10, 35K45, 37N25, 92B05

1. Introduction

In the 1970s, Keller and Segel [1, 2] studied the morphogenetic development of many species of cellular slime mold (Acrasiales), and proposed the first chemotaxis model which is called the Keller-Seger model. Since then, a vast number of results [3, 4] have been developed for the Keller-Segel models. Considering the size of the individual organism or cell, Hillen and Painter [5, 6] proposed classical chemotaxis models with a volume-filling effect. Then, in [7], they summarized the derivation and variations of the original Keller-Segel models, outlined mathematical approaches for determining global existence, and showed the instability conditions. Wang and Hillen proved that solutions exist globally in time and stay bounded for a very general class of volume-filling models in [8]. The related mathematical model with volume-filling effect can be written as

$$\begin{cases} \frac{\partial u}{\partial t} = \nabla(d_1\nabla u - \chi u(1-u)\nabla v) + g(u), \\ \frac{\partial v}{\partial t} = d_2\Delta v + \alpha u - \beta v, \end{cases} \tag{1.1}$$

where $u(x,t)$ and $v(x,t)$ are cell density and the chemical concentration at location x and time t, respectively. $d_1 > 0$ and $d_2 > 0$ represent the cell and chemical diffusion coefficients, respectively. $\chi u(1-u)\nabla v$ denotes the chemotaxis flux under a volume constraint, where 1 is defined as crowding capacity and $\chi > 0$ is called the chemotaxis coefficient. $\alpha u - \beta v$ with $\alpha, \beta > 0$ stands for the dynamic term of the chemical substances, αu implies that the chemical is secreted by cells themselves, βv is the degradation of the chemicals, and $g(u)$ is the cell kinetics term. It is classified into three cases by Mimura and Tsujikawa in [4]. (i) If $g(0) = 0$ and $g(u) < 0$ for any $u > 0$, it implies that the cells become extinct. (ii) If $g(0) = g(1) = 0$ and $g(u) > 0$ for $0 < u < 1$, the cell growth can be described by the logistic model. (iii) If $g(0) = g(\theta) = g(K) = 0$ for some $0 < K < 1$, $g(u) < 0$ for $0 < u < \theta$, and $g(u) > 0$ for $\theta < u < K$, it belongs to the bistable type.

For model (1.1) with a logistic source term, many important conclusions have been drawn in the last decade. Jiang and Zhang [9] studied the convergence of the steady state solutions of a chemotaxis model with a volume-filling effect. Ou and Yuan [10] established the existence of a traveling wavefront of a volume-filling model. Ma, Ou, and Wang [11] derived the conditions of the existence and stability of stationary solutions for a volume-filling model. Wang and Xu [12] obtained the existence of patterns by a bifurcation method. Ma and Wang [13, 14] established the global existence of classical solutions and global bifurcation for another chemotaxis model with a volume-filling effect. Ma et al. [15] investigated the emerging process and the shape of patterns for a reaction diffusion chemotaxis model with a volume-filling effect. Han et al. [16] investigated the asymptotic expressions of stationary patterns and amplitude equations near the bifurcation point for a volume-filling chemotaxis model. Ma, Gao, and Carretero-Gonzalez [17] obtained the analytical expressions of stationary patterns formation for a volume-filling chemotaxis model with a logistic growth on a two-dimensional domain.

In the present paper, we investigate the pattern formation for the following volume-filling model with a bistable source:

$$\begin{cases} \frac{\partial u}{\partial t} = \nabla(d_1\nabla u - \chi u(1-u)\nabla v) + \mu u(u-\theta)\left(1 - \frac{u}{K}\right), & x \in \Omega, t > 0, \\ \frac{\partial v}{\partial t} = d_2\Delta v + \alpha u - \beta v, & x \in \Omega, t > 0, \\ \frac{\partial u}{\partial \nu} = \frac{\partial v}{\partial \nu} = 0, & x \in \partial\Omega, t > 0, \\ u(x,0) = u_0(x), v(x,0) = v_0(x), & x \in \Omega, \end{cases} \tag{1.2}$$

where Ω is a bounded domain in $\mathbb{R}^N (N \le 3)$ with smooth boundary $\partial\Omega$, and ν is the outward unit normal vector on $\partial\Omega$. μ is the intrinsic growth rate of the cell, K represents the carrying capacity with $0 < K < 1$, and θ denotes a critical threshold of the cell density, $\theta > 0$, below which the cell becomes extinct. The homogeneous Neumann boundary conditions indicate that model (1.2) is self-contained with zero flux across the boundary. The initial data $u_0(x)$ and $v_0(x)$ are non-negative smooth functions.

This paper is organized as follows. In Section 2, we discuss the stability of equilibria of model (1.2) by local stability analysis. It is shown that the self-diffusion cannot induce spatial inhomogeneous patterns. In Section 3, sufficient conditions of destabilization are given for the steady state solution by local stability analysis. Section 4 is devoted to acquiring the process of pattern formation by weakly nonlinear analysis. We first derive the Stuart-Landau equations to capture the evolution of the amplitude of the first admissible unstable mode both in the case of supercritical and subcritical bifurcation, obtain an asymptotic expression for the stationary pattern, and show the coexisting phenomenon by the bifurcation diagram in the subcritical case. Then we acquire the competitive mechanism of the double unstable mode case. All these are verified by numerical simulation. In Section 5, the conclusion is summarized. Finally, for the completeness of the calculation process, some specific calculations are given in the two appendices at the end of this paper.

2. Linearization analysis for the semi-linear model

The local model corresponding to (1.2) can be written in the form

$$\begin{cases} \frac{du}{dt} = \mu u(u-\theta)\left(1-\frac{u}{K}\right) := f_1(u), \\ \frac{dv}{dt} = \alpha u - \beta v := f_2(u,v). \end{cases} \tag{2.1}$$

Obviously, (2.1) has three equilibria: the trivial equilibrium $E_0 = (0, 0)$, and two non-trivial equilibria $E_\theta = (\theta, \theta\alpha/\beta)$ and $E_K = (K, K\alpha/\beta)$. In the phase plane, E_0, E_θ, and E_K are collinear. The Jacobian matrices of (2.1) at E_0, E_θ, and E_K are denoted as follows, respectively:

$$J_0 = \begin{pmatrix} -\theta\mu & 0 \\ \alpha & -\beta \end{pmatrix}, \quad J_\theta = \begin{pmatrix} \theta\left(1-\frac{\theta}{K}\right)\mu & 0 \\ \alpha & -\beta \end{pmatrix}, \quad J_k = \begin{pmatrix} (\theta-K)\mu & 0 \\ \alpha & -\beta \end{pmatrix}. \tag{2.2}$$

Based on the accord Jacobian matrices at the equilibria, for the given non-negative coefficients μ, α, β, and K, the model (2.1) has the following conclusions that hold:

Theorem 2.1. (i) If $\theta \leq 0$, then the trivial equilibrium E_0 is unstable and the positive equilibrium E_K is stable; (ii) if $0 < \theta < K$, then the trivial equilibrium E_0 and the positive equilibrium E_K are stable, and another positive equilibrium E_θ is unstable.

In model (2.1), E_0 is the saddle point if $\theta \leq 0$, so cells continue to grow away from E_0. E_θ is the saddle point if $0 < \theta < K$, so cells continue to grow away from E_θ toward E_K only when cell density $u > \theta$, and when $u < \theta$, cell density continues to decrease away from E_θ toward E_0 until extinction. Since E_θ is unstable and plays the role of a separator between two stable equilibria E_0 and E_K, in the latter part, we are only concerned with E_K and E_0 when $0 < \theta < K$ holds.

The model (2.1) reflects the dynamic properties of the cell growth and changes in chemical concentrations, without considering diffusion effects. In model (1.2), let $\chi = 0$, and we get a semi-linear model as follows:

$$\begin{cases} \frac{\partial u}{\partial t} = d_1\Delta u + \mu u(u-\theta)\left(1-\frac{u}{K}\right), & x \in \Omega, t > 0, \\ \frac{\partial v}{\partial t} = d_2\Delta v + \alpha u - \beta v, & x \in \Omega, t > 0, \\ \frac{\partial u}{\partial \nu} = \frac{\partial v}{\partial \nu} = 0, & x \in \partial\Omega, t > 0, \\ u(x,0) = u_0(x),\ v(x,0) = v_0(x), & x \in \Omega. \end{cases} \tag{2.3}$$

In order to discuss model (2.3) by local stability analysis, some properties about the negative Laplace operator $-\Delta$ are given. Let $X = H^1(\Omega, \mathbb{R}^2)$ be a Sobolev space, and $\varphi(x) \in X$ be one nontrivial solution to $-\Delta\varphi = \mu_i\varphi$, $x \in \Omega$, with the homogeneous Neumann boundary condition, where

$$0 = \mu_0 < \mu_1 < \mu_2 < \cdots < \mu_i < \cdots \tag{2.4}$$

are its eigenvalues. $E(\mu_i)$ is the eigenspace corresponding to μ_i in $H^1(\Omega, \mathbb{R}^2)$, and its orthonormal basis is $\{\varphi_{ij} | j = 1, 2, \cdots, \mathrm{dimE}(\mu_i)\}$.

$$X_{ij} = \{\mathbf{C}\varphi_{ij} | \mathbf{C} \in \mathbb{R}^2\}, \quad X_i = \bigoplus_{j=1}^{\mathrm{dimE}(\mu_i)} X_{\mathrm{ij}}, \quad X = \bigoplus_{i=1}^{\infty} X_{\mathrm{i}}. \tag{2.5}$$

In particular, if $\Omega = (0, l) \subset \mathbb{R}$, then

$$\mu_i = (\pi i/l)^2, \quad i = 0, 1, 2, \cdots, \quad \varphi_i(x) = \begin{cases} 1, & i = 0, \\ \cos(\pi i x/l), i > 0. \end{cases} \tag{2.6}$$

Combining (2.4) with (2.5) and (2.6), the equilibrium E_K is transformed to the origin by the transformations $\tilde{u} = u - K$ and $\tilde{v} = v - K\alpha/\beta$. For convenience, we still denote $\tilde{u}$ and $\tilde{v}$ by u and v, respectively. The linearized system of (2.3) at E_K is

$$\frac{\partial}{\partial t}\begin{pmatrix} u \\ v \end{pmatrix} = \begin{pmatrix} \mu(\theta - k) - d_1\mu_i & 0 \\ \alpha & -\beta - d_2\mu_i \end{pmatrix}\begin{pmatrix} u \\ v \end{pmatrix} = \mathcal{L}(\mu_i)\begin{pmatrix} u \\ v \end{pmatrix}. \tag{2.7}$$

So, the characteristic equation of the model (2.7) is

$$\lambda^2 - \mathrm{Tr}(\mathcal{L}(\mu_i))\lambda + \mathrm{Det}(\mathcal{L}(\mu_i)) = 0, \tag{2.8}$$

where

$$\mathrm{Tr}(\mathcal{L}(\mu_i)) = -\beta - (d_1 + d_2)\mu_i - \mu(K - \theta),$$
$$\mathrm{Det}(\mathcal{L}(\mu_i)) = (\beta + d_2\mu_i)(d_1\mu_i + \mu(K - \theta)).$$

If $K > \theta$, then $\mathrm{Tr}(\mathcal{L}(\mu_i)) < 0$ for all $i = 0, 1, 2, \cdots$ and $\mathrm{Det}(\mathcal{L}(\mu_i)) > 0$. A similar result appears for the trivial equilibrium E_0. Then we omit the details and summarize the results:

Theorem 2.2. The positive equilibrium E_K and the trivial equilibrium E_0 of model (2.3) are asymptotically stable.

Remark 2.1. Theorem 2.2 implies that self-diffusion does not have a destabilization effect. Moreover, since $\mathrm{Tr}(\mathcal{L}(\mu_i)) \neq 0$, Hopf bifurcation cannot appear for model (2.3).

The following section will mainly discuss the effect of chemotaxis coefficient χ at equilibrium E_K in the chemotaxis model.

3. Turing instability in the chemotaxis model

In this section, we discuss chemotaxis-driven Turing instability of model (1.2). The linearized problem of (1.2) at E_K is

$$\begin{cases} \frac{\partial W}{\partial t} = \mathcal{L}(\chi)W, \ x \in \Omega, \ t > 0, \\ \frac{\partial W}{\partial \nu} = 0, \ \ x \in \partial\Omega, \ t > 0, \end{cases} \tag{3.1}$$

where

$$W = \begin{pmatrix} u \\ v \end{pmatrix}, \mathcal{D}(\chi) = \begin{pmatrix} d_1 & -\chi K(1 - K) \\ 0 & d_2 \end{pmatrix}, J_k = \begin{pmatrix} (\theta - K)\mu & 0 \\ \alpha & -\beta \end{pmatrix}, \mathcal{L}(\chi) = J_k + \mathcal{D}(\chi)\Delta.$$

According to the properties of the negative Laplace operator $-\Delta$, model (3.1) has solutions in the form of

$$W = (c_1, c_2)^T e^{i\mathbf{k}\cdot x+\lambda t},$$

where $\mathbf{k}$ is the wave vector with wave number $k = |\mathbf{k}|$ and λ is the temporal growth rate depending on k^2. Substituting this into (3.1), we have the dispersion relation

$$\lambda^2 + p(k^2)\lambda + q(k^2) = 0, \tag{3.2}$$

where

$$\begin{aligned} p(k^2) &= \beta + (K-\theta)\mu + (d_1 + d_2)k^2, \\ q(k^2) &= \beta\mu(K-\theta) + (d_1\beta + d_2\mu(K-\theta) - \chi\alpha K(1-K))k^2 + d_1 d_2 k^4. \end{aligned} \tag{3.3}$$

Notice that characteristic equation (3.2) has two solutions:

$$\lambda_{1,2} = \frac{1}{2}(-p(k^2) \pm \sqrt{p^2(k^2) - 4q(k^2)}). \tag{3.4}$$

From the local stability theory, the chemotaxis coefficient χ is solved as

$$\chi = \frac{(\sqrt{d_1\beta} + \sqrt{d_2\mu(K-\theta)})^2}{\alpha K(1-K)} \triangleq \chi_c, \tag{3.5}$$

and (3.5) holds if and only if

$$k^2 = \sqrt{\frac{\mu\beta(K-\theta)}{d_1 d_2}} \triangleq k_c^2. \tag{3.6}$$

Here, χ_c is called the critical value for chemotaxis and k_c is the critical value for the wave number. If $\chi \le \chi_c$, for all $k > 0$, then $p^2(k^2) - 4q(k^2) \le 0$ and the eigenvalues of (3.2) satisfy $\mathrm{Re}(\lambda) \le 0$, and therefore, the equilibrium E_K is locally stable. If $\chi > \chi_c$, then there exists modes k^2 such that (3.2) has two real eigenvalues with different signs, which leads $\mathrm{Re}(\lambda) > 0$ to destabilization.

Especially, if $q(k^2) = 0$, then

$$\chi = \frac{(\beta + d_2k^2)(d_1k^2 + \mu(K-\theta))}{\alpha k^2 K(1-K)} \ge \chi_c, \tag{3.7}$$

and the equal sign holds if and only if (3.6) holds.

Based on the above analysis, we obtain the following results.

Theorem 3.1. Let $K, \alpha, \beta, \mu, \theta, d_1$, and d_2 be fixed. If $\chi = \chi_c$, the equilibrium E_K of model (1.2) is neutrally stable. If $\chi > \chi_c$ and there exists modes k^2 such that

$$k_1^2 < k^2 < k_2^2, \tag{3.8}$$

then the equilibrium E_K destabilizes in the case $q(k^2) < 0$ and $q(k_i^2) = 0,\ i = 1,\ 2$, with

$$\begin{aligned} k_1^2 &= \tfrac{1}{2d_1d_2}(h - \sqrt{h^2 - 4\beta d_2\mu d_1(K-\theta)}), \\ k_2^2 &= \tfrac{1}{2d_1d_2}(h + \sqrt{h^2 - 4\beta d_2\mu d_1(K-\theta)}), \\ h &= \alpha(K-K^2)\chi - \beta d_1 - d_2\mu(K-\theta). \end{aligned} \tag{3.9}$$

Now we discuss the case at stable equilibrium E_0. The corresponding linearized operator is given by

$$\mathcal{L} = \begin{pmatrix} -\theta\mu - d_1\Delta & 0 \\ \alpha & -\beta - d_2\Delta \end{pmatrix}.$$

Referring to the deducing process of (3.2), (3.3), and (3.4), we have the following results:

Theorem 3.2. The equilibrium E_0 of model (1.2) is always locally stable, where $K, \alpha, \beta, \mu, \theta, d_1$, and d_2 are fixed. In this case, chemotaxis diffusion does not induce a pattern.

Remark 3.1. Let $\Omega = (0, l)$, and wave number $k = \frac{\pi j}{l}$, $j = 1, 2, \cdots$ for model (1.2). For $\chi \geq \chi_c$, define $K_\chi = \{k = \frac{\pi j}{l} | k_1^2 < k^2 < k_2^2,\ j \in \mathbb{N}_+\}$ to be admissible wave number sets. When χ is sufficiently greater than χ_c, then $K_\chi \neq \emptyset$. Substituting $k \in K_\chi$ into (3.7), we can define S_χ to be a set of all admissible bifurcation values, where

$$S_\chi = \{\chi | \chi = \frac{(\beta l^2 + d_2\pi^2 j^2)(d_1\pi^2 j^2 + \mu l^2(K - \theta))}{\alpha\pi^2 j^2 l^2 K(1 - K)},\ j = 1, 2, \cdots\},\ \chi_m = \min_j S_\chi, \tag{3.10}$$

and χ_m is the smallest admissible bifurcation value, $\chi_m \geq \chi_c$. The equal sign holds if and only if there exists $j_0 \in \mathbb{N}_+$ such that $\pi j_0 / l = k_c$ holds. In this case, k_c is admissible, and then $k_c \in K_\chi$. On the other hand, $S_\chi = \emptyset$ and $K_\chi = \emptyset$ when $\chi < \chi_c$.

Remark 3.2. Suppose $\chi > \chi_c$, and if at least one mode k^2 is admissible for the domain Ω and zero-Neumann boundary conditions, then a spatial pattern appears.

Remark 3.3. Since $p(k^2) \neq 0$, Hopf bifurcation cannot appear at the positive equilibrium E_K of model (1.2).

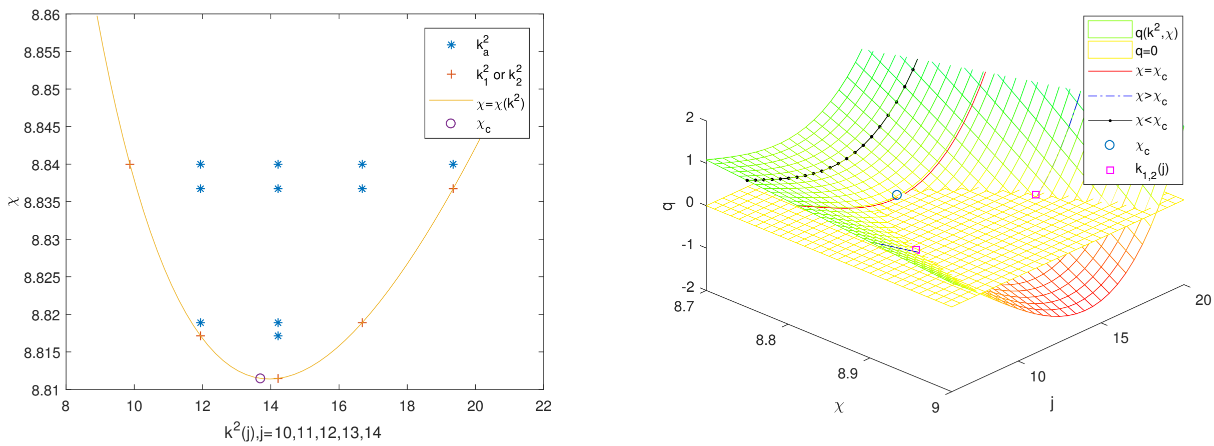

Figure 1. Left: Plot of $\chi = \chi(k^2(j))$. The yellow line represents the curve $q(k^2(j), \chi) = 0$, the horizontal and vertical coordinates of the points * are, respectively, $\chi \in S_\chi$ and unstable modes $k^2(j)$, $k(j) \in K_\chi$, and $j \in \mathbb{N}_+$. Right: The surface of $q = q(k^2(j), \chi)$. The red line, blue line, and dashed line on the surface represent $\chi = \chi_c, \chi < \chi_c$, and $\chi > \chi_c$, respectively. See Example 4.3 for details of the parameters.

Relations of mode $k^2(j)$, wave number $k(j)$, and the coefficient of chemotaxis χ are shown in Figure 1. It notes the admissible wave numbers and bifurcation values, critical wave number k_c, and bifurcation value χ_c, as well as borderline curve $\chi = \chi(k^2)$, and surface $q = q(k^2, \chi)$.

The linear stability analysis mainly discusses the behavior of the model near the equilibrium. In the following sections, we will discuss how the model may appear to have new behaviors when it leaves the equilibrium and loses stability.

4. A stationary pattern for the chemotaxis model

In this section, we will discuss the pattern solution of model (1.2) when the chemotaxis coefficient χ exceeds the critical value χ_c by weakly nonlinear analysis. The amplitude equations of the spatiotemporal patterns are established using a multiple-scale perturbation approach, and the asymptotic expressions for the stationary patterns are determined by analyzing the amplitude equations. For simplicity, let $\Omega = (0, l) \subset \mathbb{R}$.

4.1. Multiple-scale analysis

Given the linear transformations $U = u - K$, $V = v - K\beta/\theta$, and $W = (U, V)^T$, model (1.2) is rewritten as follows:

$$\begin{cases} \frac{\partial W}{\partial t} = \mathcal{L}(\chi)W + \mathcal{N}W, \ x \in \Omega, \ t > 0, \\ \frac{\partial W}{\partial \nu} = 0, \ x \in \partial\Omega, \ t > 0, \end{cases} \tag{4.1}$$

where

$$\mathcal{N}W = \left(\frac{\mu\left(U^2(\theta - 2K - U)\right)}{K} + \chi(2K + 2U - 1)\nabla U \nabla V + \chi(U(K + U - 1))\Delta V, \ 0 \right)^T.$$

We expand χ, W, and t as follows:

$$\begin{gathered} t = t(T_1, T_2, T_3, \cdots), \ T_i = \varepsilon^i t, \ i = 1, 2, 3, \cdots, \\ \chi = \chi_a + \varepsilon\chi_1 + \varepsilon^2\chi_2 + \varepsilon^3\chi_3 + \varepsilon^4\chi_4 + \varepsilon^5\chi_5 + \cdots, \\ W = \varepsilon W_1 + \varepsilon^2 W_2 + \varepsilon^3 W_3 + \varepsilon^4 W_4 + \varepsilon^5 W_5 + \cdots, \end{gathered} \tag{4.2}$$

where $W_i = (U_i, V_i)^T$, T_i, $i = 1, 2, \cdots$ represent different time scales, χ_a is the bifurcation value, and ε is a control parameter that implies the distance from χ to the bifurcation point χ_a.

Substituting (4.2) into (4.1), collecting terms at each order in ε, and comparing the coefficients of terms ε, ε^2, ε^3, ε^4, and ε^5 on both sides of the equation, we get a sequence of coefficient equations.

$$O(\varepsilon) : \mathcal{L}(\chi_a)W_1 = \mathbf{0}, \tag{4.3}$$

$$O(\varepsilon^2) : \mathcal{L}(\chi_a)W_2 = F(W_1), \tag{4.4}$$

$$O(\varepsilon^3) : \mathcal{L}(\chi_a)W_3 = G(W_1, W_2), \tag{4.5}$$

$$O(\varepsilon^4) : \mathcal{L}(\chi_a)W_4 = H(W_1, W_2, W_3), \tag{4.6}$$

$$O(\varepsilon^5) : \mathcal{L}(\chi_a)W_5 = P(W_1, W_2, W_3, W_4), \tag{4.7}$$

where $F = (F_1, F_2)^T$, $G = (G_1, G_2)^T$, $H = (H_1, H_2)^T$, and $P = (P_1, P_2)^T$.

$$\begin{cases} F_1 = \frac{\partial U_1}{\partial T_1} + \frac{\mu(2K-\theta){U_1}^2}{K} + \chi_a(1 - 2K)\nabla(U_1 \nabla V_1) + \chi_1(1 - K)\nabla^2 V_1, \\ F_2 = \frac{\partial V_1}{\partial T_1} \end{cases}$$

and

$$\begin{cases} G_1 = \frac{\partial U_2}{\partial T_1} + \frac{\partial U_1}{\partial T_2} + \frac{\mu U_1\left(U_2(4K-2\theta)+U_1^2\right)}{K} + \chi_a \nabla\left((1-2K)\left(U_1\nabla V_2 + U_2\nabla V_1\right) - U_1^2\nabla V_1\right) \\ \quad +\chi_1\nabla\left((1-2K)\left(U_1\nabla V_1\right) + (1-K)K\nabla V_2\right) + \chi_2(1-K)K\nabla^2 V_1, \\ G_2 = \frac{\partial V_2}{\partial T_1} + \frac{\partial V_1}{\partial T_2}. \end{cases}$$

The explicit expression of H, P and all the detailed calculations are given in Appendix I.

4.2. A stationary pattern under small perturbations

Since Eqs (4.3)–(4.7) satisfy the Neumann boundary conditions, let $k_a \in K_\chi$ and $\chi_a \in S_\chi$ be the first admissible wave number and the smallest admissible bifurcation value, respectively, so we consider the solution of (4.3) as the following:

$$W_1 = A(T_1,\ T_2)\cos(k_a x)\rho, \quad \rho = \begin{pmatrix} M \\ 1 \end{pmatrix}, \tag{4.8}$$

where $M = \frac{\beta + d_2 k_a^2}{\alpha}$, $\rho \in \mathrm{Ker}(\mathcal{L}(\chi_a))$, and A is the amplitude function depending only on the time scales $T_i,\ i = 1, 2, \cdots$.

Substituting W_1 into $F(W_1)$, leads to

$$\begin{cases} F_1 = \frac{\partial A}{\partial T_1} M\cos(k_a x) + \frac{A^2\mu M^2(2K-\theta)}{2K} - \chi_1 A(K-K^2)k_a^2\cos(k_a x) \\ \quad +\frac{A^2 M\left((4K^2-2K)k_a^2\chi_a + \mu M(2K-\theta)\right)\cos(2k_a x)}{2K}, \\ F_2 = \frac{\partial A}{\partial T_1}\cos(k_a x). \end{cases}$$

Let L^* be the adjoint operator of $\mathcal{L}(\chi_a)$. A fundamental solution of $L^* w^* = 0$ is given as follows:

$$w^* = (M^*, 1)^T\cos(k_a x), \quad M^* = \frac{\alpha}{\mu(K-\theta) + d_1 k_a^2}. \tag{4.9}$$

According to the Fredholm theorem, the solvability condition of (4.4) is

$$\int_0^l F\cdot w^*\,dx = 0,\ l = \frac{j\pi}{k_a},\ j \in \mathbb{N}_+,$$

and then we obtain

$$\frac{\partial A}{\partial T_1} = \frac{\chi_1(K-K^2)M^* k_a^2}{1 + MM^*}A. \tag{4.10}$$

Since A is the amplitude of the slow change in the time scales $T_1,\ T_2, \cdots$, but the solution of (4.10) increases rapidly with T_1, then we take $\chi_1 = 0$ and $T_1 = 0$, so that $\frac{\partial A}{\partial T_1} = 0$, and it implies independence between solutions and time scales T_1. From this, the solution of (4.4) can be represented in the form

$$W_2 = A^2(a_{21},\ b_{21})^T + A^2(a_{22},\ b_{22})^T\cos(2k_a x). \tag{4.11}$$

By substituting (4.11) into (4.4), the following expression is obtained:

$$\begin{aligned} &a_{21} = \frac{M^2(\theta-2K)}{2K(K-\theta)},\ a_{22} = M\left(4d_2k_a^2 + \beta\right)s,\ b_{21} = -\frac{\alpha M^2(2K-\theta)}{2\beta K(K-\theta)},\ b_{22} = M\alpha s, \\ &s = -\frac{\left(4K^2-2K\right)k_a^2\chi_a + \mu M(2K-\theta)}{2K\left(\left(4d_2k_a^2+\beta\right)\left(4d_1k_a^2 + \mu(K-\theta)\right) - 4\alpha\left(K-K^2\right)k_a^2\chi_a\right)}. \end{aligned}$$

Combining (4.8), (4.11), and (4.5), noting $\chi_1 = 0$, $T_1 = 0$, $\frac{\partial W}{\partial T_1} = 0$, and $\frac{\partial W}{\partial T_3} = 0$, then G is rewritten as follows:

$$\begin{cases} G_1 = \frac{\partial A}{\partial T_2} M\cos(k_a x) + (AG_{11} + A^3 G_{12})\cos(k_a x) + A^3 G_{13}\cos(3k_a x), \\ G_2 = \frac{\partial A}{\partial T_2}\cos(k_a x), \end{cases}$$

where

$$\begin{aligned} G_{11} &= (K - K^2)\chi_2 k_a^2, \\ G_{12} &= \tfrac{1}{4K}(\mu M(3M^2 + 4(2K-\theta)(2a_{21} + a_{22})) + Kk_a^2\chi_a(4K-2)(2Mb_{21} + 2a_{21} - a_{22}) + M^2)), \\ G_{13} &= \tfrac{1}{4K}(3Kk_a^2\chi_a((4K-2)(a_{22} - 2Mb_{21}) + M^2) + M\mu(4a_{22}(2K-\theta) + M^2)). \end{aligned}$$

By the Fredholm solvability condition $\int_0^l G \cdot w^* \, dx = 0$, $l = \frac{j\pi}{k_a}$, $j \in \mathbb{N}_+$, and the cubic Stuart-Landau equation of amplitude A is obtained as follows:

$$\frac{dA}{dT_2} = \sigma A - LA^3, \tag{4.12}$$

where

$$\begin{aligned} \sigma &= \frac{(1-K)KM^*\chi_2 k_a^2}{MM^*+1}, \\ L &= \frac{M^*(Kk_a^2\chi_a((4K-2)(2Mb_{21}+2a_{21}-a_{22})+M^2)+\mu M(4(2a_{21}+a_{22})(2K-\theta)+3M^2))}{4K(MM^*+1)}. \end{aligned} \tag{4.13}$$

Obviously, $\sigma > 0$, and we obtain the following result.

Theorem 4.1. Let $\mu, \alpha, \beta, \theta, K, d_1$, and d_2 be fixed. If $L > 0$, then (4.12) is supercritical. If $L < 0$, then (4.12) is subcritical.

Due to the complexity of the L expression, it is very difficult to analyze its positivity or negativity in the parameter space. Figure 2 gives supercritical and subcritical bifurcation diagrams on the phase planes (μ, K) and (θ, K), respectively, for a given parameter. In the following, we respectively derive asymptotic expressions about the evolution of the spatiotemporal pattern for the supercritical and subcritical cases.

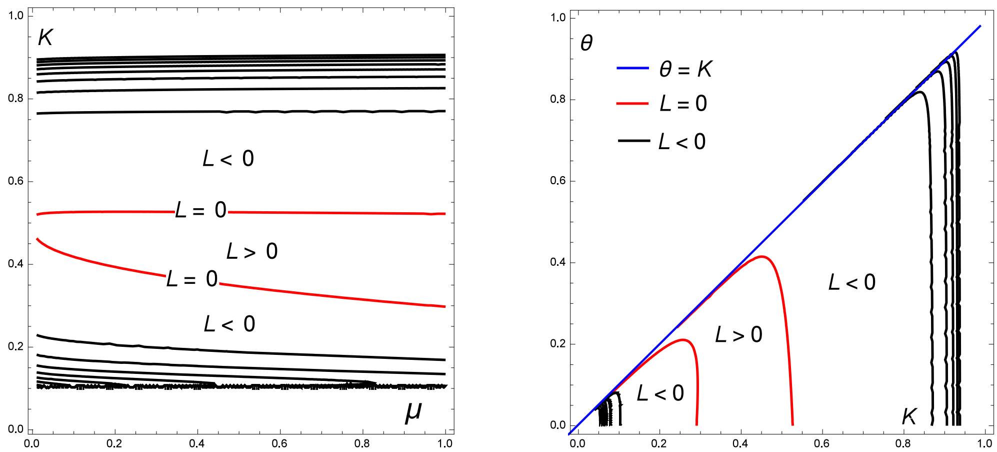

Figure 2. The $L > 0$ regions represent the supercritical case, the $L < 0$ regions correspond to the subcritical case, and the red curves are the bifurcation lines. The parameters are taken as $d_1 = 1.5, d_2 = 0.1, \beta = 35$, and $\alpha = 35$. The left figure is the $\mu - K$ phase diagram, and the right figure is the $K - \theta$ phase diagram with parameters $\theta = 0.1$ and $\mu = 0.1$, respectively.

4.2.1. The supercritical case

Since $\frac{\partial W_1}{\partial T_1} = 0$, the amplitude A in (4.12) only depends on time scale T_2. Considering the cubic Stuart-Landau equation (4.12) subject to initial data $A(0) = A_0$, we have

$$A(T_2) = \frac{1}{\sqrt{e^{-2\sigma T_2}\left(\frac{1}{A_0^2} - \frac{L}{\sigma}\right) + \frac{L}{\sigma}}}.$$

Substituting $A(T_2)$, (4.8), and (4.11) into (4.2), one can express the spatiotemporal pattern $W(t, x)$ at $O(\varepsilon^3)$ as follows:

$$W(t, x) = \varepsilon A(t)\begin{pmatrix} M \\ 1 \end{pmatrix}\cos(k_a x) + \varepsilon^2 A^2(t)\begin{pmatrix} a_{21} & a_{22} \\ b_{21} & b_{22} \end{pmatrix}\begin{pmatrix} 1 \\ \cos(2k_a x) \end{pmatrix} + O(\varepsilon^3). \tag{4.14}$$

It is easy to verify that the unique positive equilibrium $\sqrt{\sigma/L}$ is asymptotically stable when $\sigma > 0$ and $L > 0$:

$$\lim_{T_2 \to +\infty} A(T_2) = \sqrt{\sigma/L} \triangleq A_\infty.$$

Base on the above analysis, we get the following conclusion.

Remark 4.1. Consider model (1.2) in $\Omega = (0, l)$ and parameters $(\mu, \alpha, \beta, \theta, K, d_1, d_2)$ are fixed. Assume $\chi > \chi_c$ and there is only one admissible wave number $k_a \in K_\chi$ when the control parameter $\varepsilon^2 = (\chi - \chi_a)/\chi_a$ is small enough. If L is positive, then we have the second-order asymptotic expression of the stationary pattern near the equilibrium E_K as follows:

$$\begin{pmatrix} u(x) \\ v(x) \end{pmatrix} = \begin{pmatrix} K \\ \frac{K\alpha}{\beta} \end{pmatrix} + \varepsilon A_\infty \begin{pmatrix} M \\ 1 \end{pmatrix}\cos(k_a x) + \varepsilon^2 A_\infty \begin{pmatrix} a_{21} & a_{22} \\ b_{21} & b_{22} \end{pmatrix}\begin{pmatrix} 1 \\ \cos(2k_a x) \end{pmatrix} + O(\varepsilon^3). \tag{4.15}$$

Remark 4.2. Substituting σ, L, and $\chi_2 = (\chi - \chi_a)/\varepsilon^2$ into $\sqrt{\sigma/L} = A_\infty$, we have the supercritical bifurcation curve as follows:

$$\chi = \chi_a + \frac{L(MM^* + 1)\varepsilon^2}{K(1-K)M^* k_a^2} A_\infty^2.$$

Its bifurcation diagram is shown in the red curve on the left of Figure 3.

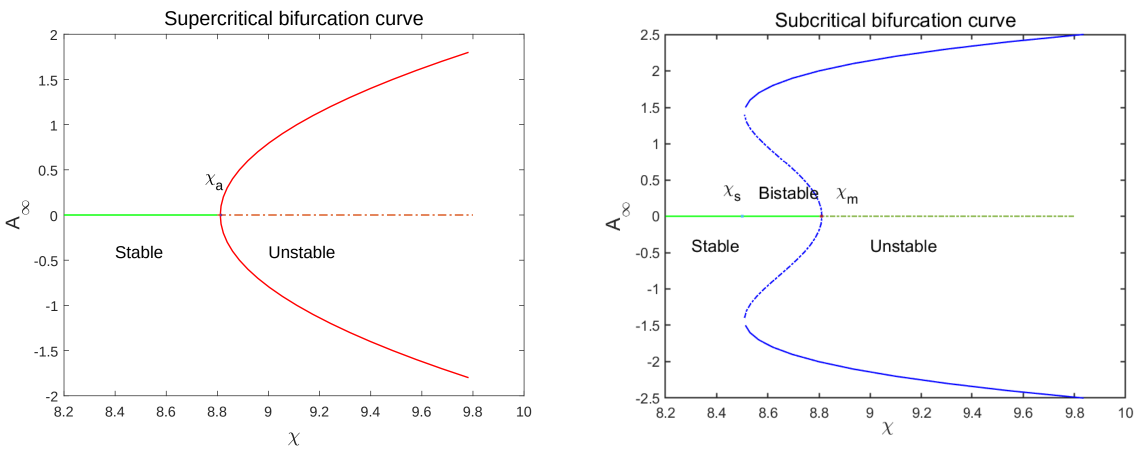

Figure 3. Left: The red curve is the supercritical bifurcation curve. Right: The blue curve represents the subcritical bifurcation curve, and (χ_s, χ_m) is the bistable interval.

Example 4.3. *We choose coefficients in model (1.2) as follows:*

$$\mu = 0.7,\ \theta = 0.1,\ \beta = 35,\ d_1 = 1.5,\ d_2 = 0.1,\ \alpha = 35,\ K = 0.5,\ l = 2\pi.$$

It is easy to obtain the positive equilibrium $E_K = (0.5, 0.5)$, the chemotaxis critical value $\chi_c = 6.28033 \notin S_\chi$, and critical wave number $k_c = 2.84304 \notin K_\chi$. Set $\chi = 6.29603$ and $\chi = 6.3413$, the corresponding control parameters are $\varepsilon = 0.05$ and $\varepsilon = 0.1$, respectively, the conditions of Theorem 3.1 holds, and E_K destabilizes. Further, we take the bifurcation value $\chi_a = 6.28954$ and the first admissible wave number $k_a = 3$, and then $\chi_2 = \frac{\chi-\chi_a}{\varepsilon^2}$, $\sigma > 0$, and $L > 0$, so Example 4.3 belongs the supercritical case. The corresponding second-order asymptotic expression of the stationary pattern is given as follows:

$$\begin{cases} u(x) = 0.491287 + 0.062227\cos(3x) - 0.0008055\cos(6x) + O(\varepsilon^2), \\ v(x) = 0.491287 + 0.060667\cos(3x) - 0.0007304\cos(6x) + O(\varepsilon^2), \end{cases} \quad \varepsilon = 0.05,\ \chi = 6.29603,$$

$$\begin{cases} u(x) = 0.478676 + 0.097351\cos(3x) - 0.0021095\cos(6x) + O(\varepsilon^2), \\ v(x) = 0.478676 + 0.095967\cos(3x) - 0.0020108\cos(6x) + O(\varepsilon^2), \end{cases} \quad \varepsilon = 0.1,\ \chi = 6.34313.$$

To illustrate the correctness of the asymptotic expression, we give numerical solutions for Example 4.3. In Figure 4, we have a comparison between the numerical solution and the weakly nonlinear asymptotic solution of Example 4.3. Of these, the absolute deviation (|WNS-NS|) is approximately less than 1.5%.

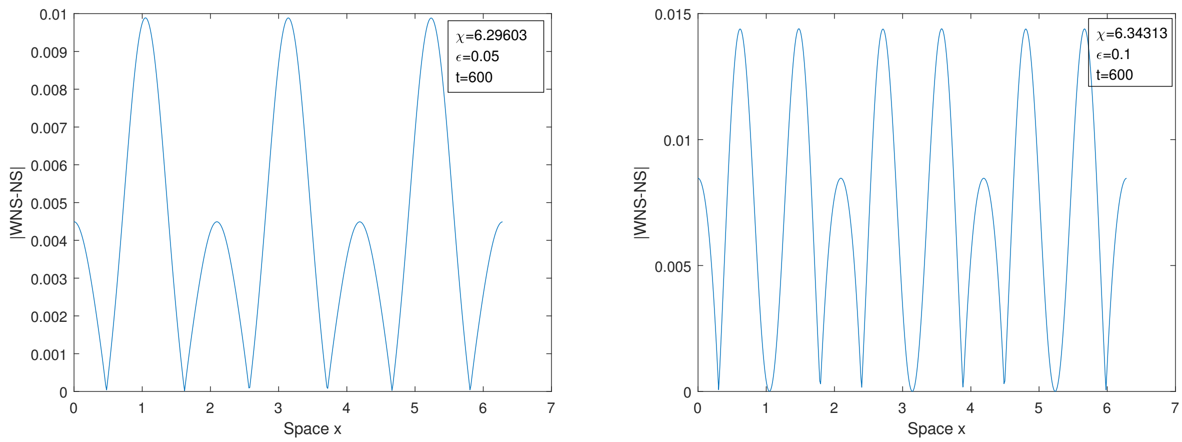

Figure 4. Comparison between the weakly nonlinear solution (WNS) and the numerical solution (NS) of Example 4.3, i.e., |WNS-NS|. The initial data is set as a 0.1% random small perturbation of the $(K, K\alpha/\beta)$.

4.2.2. The subcritical case

If $L < 0$, the unique equilibrium $A = 0$ of the cubic Stuart-Landau equation (4.12) is unstable. The amplitude equation lacks a saturation term to limit the amplitude development, so a higher-order perturbation term should be introduced for analysis.

Therefore, we push the weakly nonlinear expansion to $O(\varepsilon^5)$, and get the quintic Stuart-Landau equation for the amplitude as follows:

$$\frac{dA}{dT} = \bar{\sigma}A - \bar{L}A^3 + \bar{Q}A^5, \tag{4.16}$$

where

$$\bar{\sigma} = \sigma + \varepsilon^2\tilde{\sigma},\ \bar{L} = L + \varepsilon^2\tilde{L},\ \bar{Q} = \varepsilon^2\tilde{Q}, \tag{4.17}$$

and σ and L are given in (4.13). W_3, W_4, $\tilde{\sigma}$, $\tilde{L}$, and $\tilde{Q}$ are deduced at the same time. The detailed calculations are given by (A.3), (A.6), and (A.9) in Appendix I.

Substituting W_1, W_2, W_3, W_4, and $A(t)$ into Eq (4.2), we obtain the explicit approximation of the spatiotemporal pattern $W(x,t)$ at $O(\varepsilon^5)$:

$$\begin{aligned} W(t,x) &= \varepsilon W_1 + \varepsilon^2 W_2 + \varepsilon^3 W_3 + \varepsilon^4 W_4 + O(\varepsilon^5) \\ &= \varepsilon A\begin{pmatrix} M \\ 1 \end{pmatrix}\cos(k_a x) + \varepsilon^2 A^2 \begin{pmatrix} a_{21} & a_{22} \\ b_{21} & b_{22} \end{pmatrix}\begin{pmatrix} 1 \\ \cos(2k_a x) \end{pmatrix} \\ &+ \varepsilon^3 A \begin{pmatrix} a_{31} + A^2 a_{32} & a_{33} \\ b_{31} + A^2 b_{32} & b_{33} \end{pmatrix}\begin{pmatrix} \cos(k_a x) \\ A^2\cos(3k_a x) \end{pmatrix} \\ &+ \varepsilon^4 A^2 \begin{pmatrix} a_{41} + a_{42}A^2 & a_{43}A^2 + a_{44} & a_{45} \\ b_{41} + b_{42}A^2 & b_{43}A^2 + b_{44} & b_{45} \end{pmatrix}\begin{pmatrix} 1 \\ \cos(2k_a x) \\ A^2\cos(4k_a x) \end{pmatrix} + O(\varepsilon^5), \end{aligned} \tag{4.18}$$

where all coefficients are expressed in Appendix I.

In this subcritical case, since $\bar{\sigma} > 0$ and $\bar{L} > 0$, when $\bar{Q} < 0$, it is easy to prove that quintic Stuart-Landau equation (4.16) has a globally asymptotically stable solution:

$$A_\infty = \lim_{T\to+\infty} A(T) = \sqrt{\frac{\bar{L} - \sqrt{\bar{L}^2 - 4\bar{\sigma}\bar{Q}}}{2\bar{Q}}}. \tag{4.19}$$

By substituting A_∞ into (4.18), the fourth-order weakly nonlinear asymptotic expression of the stationary pattern is given:

$$\begin{pmatrix} u(x) \\ v(x) \end{pmatrix} = \begin{pmatrix} K \\ \frac{K\alpha}{\beta} \end{pmatrix} + \lim_{t\to+\infty} W(x,t) + O(\varepsilon^5). \tag{4.20}$$

Example 4.4. *Choose coefficients in model (1.2) as follows:*

$$\mu = 0.2,\ \theta = 0.2,\ d_1 = 2,\ d_2 = 0.4,\ \alpha = 20,\ \beta = 20,\ K = 0.6,\ l = 10\pi.$$

Then, $E_K = (0.6, 0.6)$*,* $\chi_c = 8.81140452 \notin S_\chi$*,* $k_c = 1.18921 \notin K_\chi$*, and* $\chi_m = 8.81148148$*. We take* $\chi_a = 8.81714876$*,* $k_a = 1.2$*,* $\chi = 8.89951$*, and* $\varepsilon = 0.1$*. All conditions of Theorem 3.1 are satisfied, and the positive equilibrium* E_K *is unstable. Further* $\bar{\sigma} = 2.39871$*,* $\bar{L} = -8.75287$*, and* $\bar{Q} = -2.16447$*. Eq (4.16) has a stable equilibrium* $A_\infty = 2.07401$*, so this case is the subcritical. One can reduce the Example 4.4 to the form of (4.18).*

By solving for $\chi(A_\infty)$ from (4.19), the subcritical bifurcation curve can be written in the form:

$$\chi(A_\infty) = 8.81148148 - 0.299801A_\infty^2 + 0.0741941A_\infty^4.$$

The right of Figure 3 illustrates that there exist two extreme points χ_m and χ_s, where χ_m is the root of $\chi(A_\infty) = 0$ and χ_s is the root of $\bar{L}^2 - 4\bar{\sigma}\bar{Q} = 0$. According to the calculation, we have

$$\chi_s = 8.50862505, \chi_m = 8.81148148.$$

In the example, there are two stable branches coexisting at $\chi \in (\chi_s, \chi_m)$, which are called bistability. The two essential ingredients for bistable behavior are nonlinearity and feedback [18]. Suppose that χ is increased from some value less than χ_s. For any given small amplitude perturbation around E_K, the steady state remains until $\chi = \chi_m$, where the E_K loses stability. Namely, while χ_m is exceeded, the solution jumps to the stable equilibrium with large amplitude. By the same method, for the stable branch with larger amplitude, the jump exists at $\chi = \chi_s$. In this way, a bistable interval is given, as depicted in Figure 3. The solution around equilibrium sensitively depends on the initial conditions. We respectively take initial perturbations of different amplitudes $A = 0.1$ and $A = 0.2$ at $\chi = 8.735059 \in (\chi_s, \chi_m)$, which induce different patterns. The left of Figure 5 shows a critical case of the uniform equilibrium rapidly turning to the spatiotemporal pattern at a given small amplitude initial perturbation. The right of Figure 5 shows that stationary pattern W expressed by (4.18) is reached at a given initial perturbation of large amplitude. According to the analysis, we have the following result.

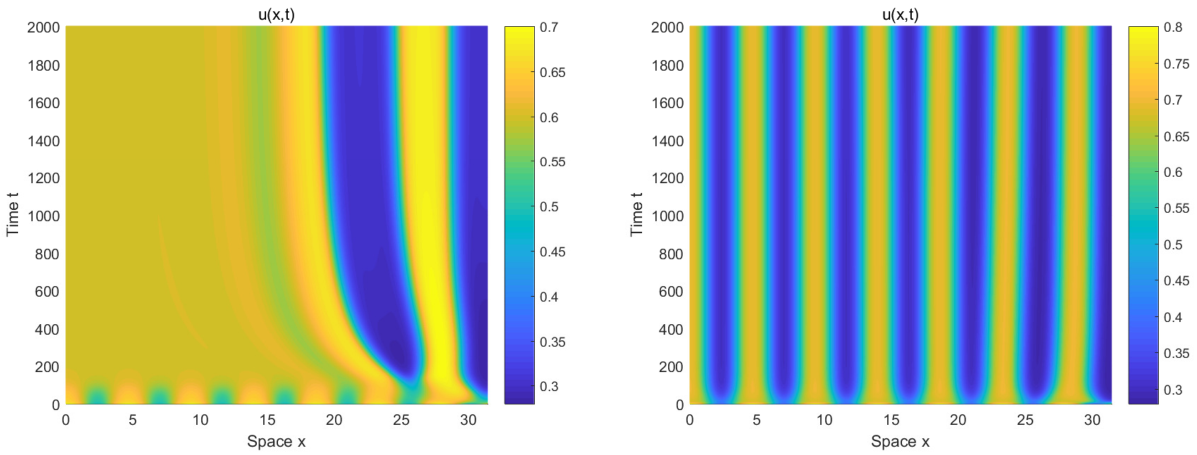

Figure 5. Two equilibriums coexist at $\chi = 8.735059 \in (\chi_s, \chi_m)$ in the Example 4.4. Left: The initial value $u_0 = 0.6 + 0.1\cos(1.35x)$. Right: The initial value $u_0 = 0.6 + 0.2\cos(1.35x)$.

4.3. A stationary pattern for large perturbations

Previously, we discussed the stationary pattern of model (1.2) when the equilibrium E_K loses stability if given bifurcation parameter $\chi > \chi_c$, and χ deviates χ_a small enough to have a unique unstable mode $k_a \in K_\chi$, i.e., control parameter ε is small enough. In this section, we derive how the unstable modes interact and how to determine the shape of the stationary pattern while ε is large enough to have two unstable modes for model (1.2) with $\Omega = (0, l)$. According to Theorem 3.1 and Remark 3.1, we have the following conclusion.

Theorem 4.2. Set $\chi_{m_i} \in S_\chi$, $i = 1, 2, 3, \cdots$, and $\chi_c \le \chi_m = \chi_{m_1} < \chi_{m_2} < \chi_{m_3} < \cdots$. If $\chi > \chi_{m_2}$, then there exist at least two unstable modes for given chemotaxis coefficient χ.

Proof. By the definition of S_χ, since $\chi_m \in S_\chi$, then there exists a $j_1 \in \mathbb{N}_+$ such that

$$k_{j_1} = \frac{j_1 \pi}{l}, \quad \chi_m = \frac{(\beta l^2 + d_2 \pi^2 j_1^2)(d_1 \pi^2 j_1^2 + \mu l^2 (K - \theta))}{\alpha \pi^2 j_1^2 l^2 K (1 - K)}, \quad q(k_{j_1}^2, \chi_m) = 0.$$

Similarly, for $\chi_{m_2} \in S_\chi$, there exists a $j_2 \in \mathbb{N}_+$ such that

$$k_{j_2} = \frac{j_2\pi}{l},\ \ \chi_{m_2} = \frac{(\beta l^2 + d_2\pi^2 j_2^2)(d_1\pi^2 j_2^2 + \mu l^2(K-\theta))}{\alpha\pi^2 j_2^2 l^2 K(1-K)},\ \ q(k_{j_2}^2, \chi_{m_2}) = 0.$$

So if $\chi > \chi_{m_2}$, wave numbers k_{j_1} and k_{j_2} are in sets K_χ, i.e., $q(k_{j_1}^2, \chi) < 0$ and $q(k_{j_2}^2, \chi) < 0$. This implies that $k_{j_1}^2$ and $k_{j_2}^2$ are unstable modes of χ. □

Based on the above analysis, we investigate the competitive law between unstable modes k_1^2 and k_2^2 by deriving their amplitude equations. Then we set the solution of (4.3) in the following form:

$$W_1 = A_1(M_1, 1)^T \cos(k_1 x) + A_2(M_2, 1)^T \cos(k_2 x), \tag{4.21}$$

where A_i's only depending temporal variable is the amplitude of modes k_i^2 with $i = 1, 2$ and

$$M_1 = \frac{\beta + d_2 k_1^2}{\alpha},\ \ M_2 = \frac{\beta + d_2 k_2^2}{\alpha}.$$

Substituting (4.21) into (4.4) and (4.5), and combining with the Fredholm theorem, we obtain the following ODE model of the amplitude:

$$\begin{cases} \frac{dA_1}{dT} = \tau_1 A_1 - L_1 A_1^3 + Q_1 A_1 A_2^2, \\ \frac{dA_2}{dT} = \tau_2 A_2 - L_2 A_2^3 + Q_2 A_2 A_1^2, \end{cases} \tag{4.22}$$

where the explicit expressions of $\tau_i,\ L_i$, and $Q_i,\ i = 1, 2$, are presented in Appendix II. Obviously, $\tau_i > 0,\ i = 1, 2$. Under the conditions $L_i > 0,\ i = 1, 2$ and

$$L_2\tau_1 - Q_1\tau_2 < 0, \quad L_1\tau_2 - Q_2\tau_1 < 0, \quad L_1L_2 - Q_1Q_2 < 0. \tag{4.23}$$

Model (4.22) has four non-negative equilibria in the first quadrant:

$$E_1\ (0,0),\quad E_2\ (\sqrt{\frac{\tau_1}{L_1}}, 0),\quad E_3\ (\sqrt{\frac{\tau_2}{L_2}}, 0),\quad E_4\ (\sqrt{\frac{L_2\tau_1 - Q_1\tau_2}{L_1L_2 - Q_1Q_2}}, \sqrt{\frac{L_1\tau_2 - Q_2\tau_1}{L_1L_2 - Q_1Q_2}}\ ).$$

By linearization analysis, we know that E_1 is an unstable node, E_2 and E_3 are stable nodes, and E_4 is a saddle point. These points divide the first quadrant of the phase plane of the amplitude $A_1,\ A_2$ into four regions when (4.23) holds. Outgoing trajectories in these areas point to one of two. So we have $A_{1\infty} = \sqrt{\frac{\tau_1}{L_1}}$ and $A_{2\infty} = \sqrt{\frac{\tau_2}{L_2}}$. Let $W_2 = (U_2, V_2)^T$, and U_2 and V_2 satisfy

$$\begin{aligned} U_2 &= A_1^2(F_{11} + F_{12}\cos(2k_1x)) + A_2^2(F_{13} + F_{14}\cos(2k_2x)) + A_2A_1(F_{15}\cos((k_1 - k_2)x) \\ &\quad + F_{16}\cos((k_1 + k_2)x)), \\ V_2 &= A_1^2(F_{21} + F_{22}\cos(2k_1x)) + A_2^2(F_{23} + F_{24}\cos(2k_2x)) + A_2A_1(F_{25}\cos((k_1 - k_2)x) \\ &\quad + F_{26}\cos((k_1 + k_2)x)), \end{aligned} \tag{4.24}$$

where the coefficients are given in Appendix II (B.2). Therefore, the second-order stationary pattern with amplitude $(A_{1\infty}, A_{2\infty})$ for the double unstable modes is as follows:

$$\begin{pmatrix} u(x) \\ v(x) \end{pmatrix} = \begin{pmatrix} K \\ \frac{K\alpha}{\beta} \end{pmatrix} + \lim_{t\to+\infty}(\varepsilon W_1 + \varepsilon^2 W_2) + O(\varepsilon^3). \tag{4.25}$$

Example 4.5. *The coefficients of the given model (1.2) are chosen the same as in Example 4.3 except* $\varepsilon = 0.04$.

According to Theorem 4.2, we have $\chi_{m_1} = 6.28193$ with $j_{m_1} = 6$, $\chi_{m_2} = 6.28954$ with $j_{m_2} = 5$, and $\chi_{m_3} = 6.30463$. Set $\chi = 6.29961 > \chi_{m_2}$. So two unstable modes $k_1^2 = 2.5^2$ and $k_2^2 = 3^2$ are obtained. According to the formulas given by Appendix II (B.1)–(B.3), we have

$$\tau_1 = 7.58515,\ L_1 = 5.3335,\ Q_1 = -21.6646,\ \tau_2 = 10.9226,\ L_2 = 28.3028,\ Q_2 = -7.18535,$$

and the four non-negative equilibria are E_1 $(0,0)$, E_2 $(1.19319,0)$, E_3 $(0,1.23366)$, E_4 $(0.563221,0.521921)$. Their stability is consistent with the above analysis. Then, $A_{1\infty} = 1.19319$ and $A_{2\infty} = 1.23366$. If we take the initial data $(1.2,0.8)$, which corresponds to the P point in Figure 6, and its trajectory is attracted to the equilibrium E_2 $(A_{1\infty},0)$. The stationary pattern, the detailed comparison between the numerical solution of model (1.2), and weakly nonlinear solution (4.25) are presented in Figure 7. While the trajectory of the initial point $Q = (0.6,1.2)$ is attracted to the equilibrium E_3 $(0,A_{2\infty})$, and corresponds to the stationary pattern, the comparison between the numerical solution of model (1.2) and the weakly nonlinear solution (4.25) are presented in Figure 8.

When the bifurcation parameter χ is far enough away from the critical value χ_c, there exists a competition among two unstable modes. If we perturb the equilibrium E_K by different initial data, different stationary patterns are induced. However, after a long period of evolution, one of the unstable modes will be reduced to extinction, and another will perform a critical role in the competition of unstable modes.

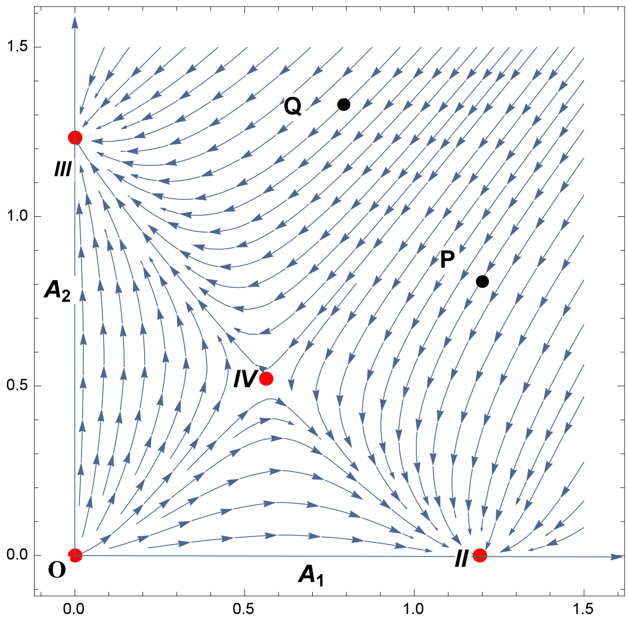

Figure 6. Some trajectories in the A_1OA_2 plane and equilibria of the amplitude equations (4.22) with the coefficients of Example 4.5.

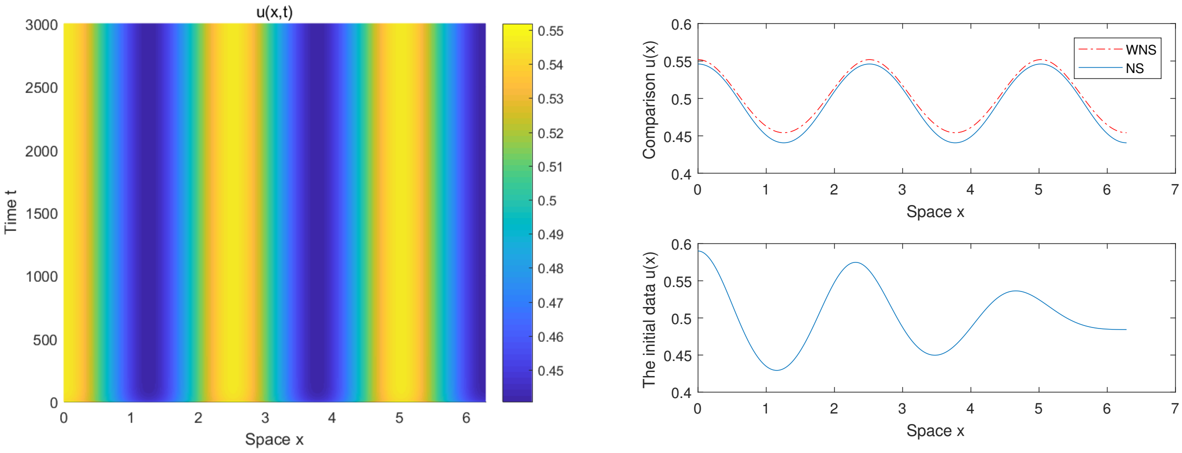

Figure 7. Left: The spatiotemporal pattern of the transition from initial amplitude P point to the stable state $(A_{1\infty}, 0)$. Right: The lower panel is the initial condition $u = E_K + \varepsilon W_1$, where $(A_1, A_2) = (1.2, 0.8)$ is attracted to the equilibrium $(A_{1\infty}, 0)$, denoted by P in Figure 6. The higher panel is the comparison between the weakly nonlinear solution (4.25 WNS) and the numerical solution (NS) of Example 4.5 about point P.

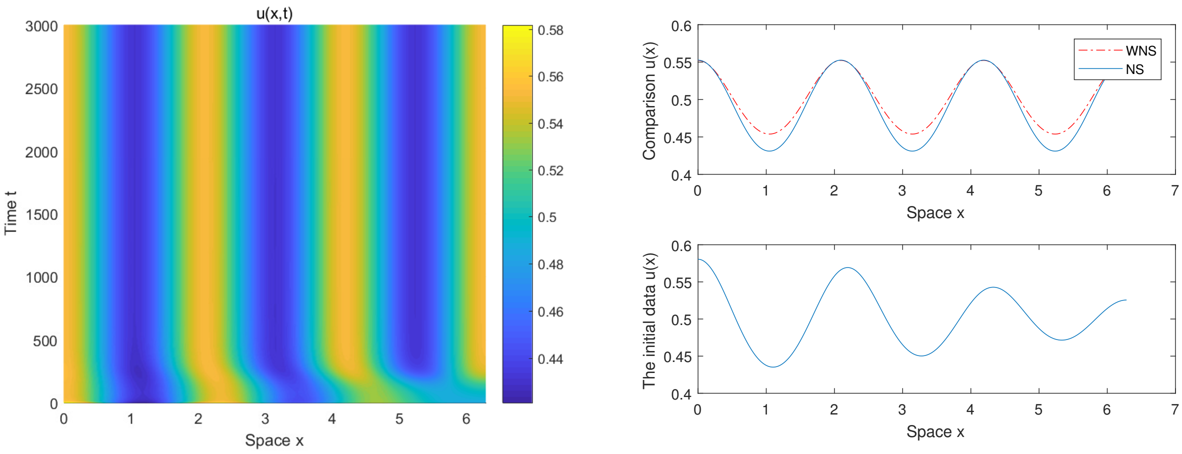

Figure 8. Left: The spatiotemporal pattern of the transition from initial amplitude Q point to the stable state $(0, A_{2\infty})$. Right: The lower panel is the initial condition $u = E_K + \varepsilon W_1$, where $(A_1, A_2) = (0.6, 1.2)$ is attracted to the equilibrium $(0, A_{2\infty})$, denoted by Q in Figure 6. The higher panel is the comparison between the weakly nonlinear solution (4.25 WNS) and the numerical solution (NS) of Example 4.5 about point Q.

5. Concluding remarks

The mechanism of the emerging process in the pattern formation has been systematically analyzed for the model (1.2) in this paper. It has been verified that some chemotaxis flux can induce pattern formation, while self-diffusion does not. The dynamics of model (1.2) is similar to the logistic model [16] if $\theta \leq 0$, where the model develops a Turing pattern when the chemotaxis coefficient $\chi > \chi_c$. Whereas if $0 < \theta < K$, two stable constant steady state solutions, E_0 and E_K, are separated. When the cell density $u < \theta$, E_0 is attractive and chemotaxis cannot induce a Turing pattern, so the cells tend to extinction. When $u > \theta$, a Turing pattern occurs in the model as the chemotaxis coefficient increases until $\chi > \chi_c$. Decreasing the threshold θ of cell density and increasing the chemotaxis coefficient are important methods to keep the cells growing and to induce a Turing pattern, respectively.

Acknowledgments

The author would like to thank the associate editor and the anonymous reviewer for their valuable comments and suggestions, which have led to a significant improvement of the whole manuscript.

Conflict of interest

The author declares no conflict of interest.

References

1. E. F. Keller, L. A. Segel, Initiation of slime mold aggregation viewed as an instability, *J. Theor. Biol.*, **26** (1970), 399–415. https://doi.org/10.1016/0022-5193(70)90092-5
2. E. F. Keller, L. A. Segel, Model for chemotaxis, *J. Theor. Biol.*, **30** (1971), 225–234. https://doi.org/10.1016/0022-5193(71)90050-6
3. D. Horstmann, From 1970 until present: the Keller-Segel model in chemotaxis and its consequences I, *Jahresbericht der Deutschen Mathematiker-Vereinigung*, **105** (2003), 103–165.
4. M. Mimura, T. Tsujikawa, Aggregating pattern dynamics in a chemotaxis modeling includeing growth, *Physica A*, **230** (1996), 499–549. http://doi.org/10.1016/0378-4371(96)00051-9
5. T. Hillen, K. J. Painter, Global existence for a parabolic chemotaxis model with prevention of overcrowding, *Adv. Appl. Math.*, **26** (2001), 280–301. http://doi.org/10.1006/aama.2001.0721
6. K. J. Painter, T. Hillen, Voluming-filling and quorum-sensing in models for chemosensitive movement, *Canadian Applied Mathematics Quarterly*, **10** (2002), 501–543.
7. T. Hillen, K. J. Painter, A user's guide to PDE models for chemotaxis, *J. Math. Biol.*, **58** (2009), 183–217. https://doi.org/10.1007/s00285-008-0201-3
8. Z. A. Wang, T. Hillen, Classical solutions and pattern formation for a volume filling chemotaxis model, *Chaos*, **17** (2007), 037108. https://doi.org/10.1063/1.2766864
9. J. Jiang, Y. Y. Zhang, On converge to equilibria for a chemotaxis model with volume-filling effect, *Asymptotic Anal.*, **65** (2009), 79–102. https://doi.org/10.3233/asy-2009-0948
10. C. H. Ou, W. Yuan, Traveling wavefronts in a volume-filling chemotaxis model, *SIAM. J. Appl. Dyn. Syst.*, **8** (2009), 390–416. http://doi.org/10.1137/08072797X
11. M. J. Ma, C. H. Ou, Z. A. Wang, Stationary solutions of a volume-filling chemotaxis model with logistic growth and their stability, *SIAM. J. Appl. Math.*, **72** (2012), 740–766. http://doi.org/10.1137/110843964

12. X. F. Wang, Q. Xu, Spiky and transition layer steady states of chemotaxis systems via global bifurcation and Helly's compactness theorem, *J. Math. Biol.*, **66** (2013), 1241–1266. http://doi.org/10.1007/s00285-012-0533-x
13. M. J. Ma, Z. A. Wang, Global bifurcation and stablility of steady states for a reaction-diffusion-chemotaxis model with volume-filling effect, *Nonlinearity*, **28** (2015), 2639–2660. http://doi.org/10.1088/0951-7715/28/8/2639
14. M. J. Ma, Z. A. Wang, Patterns in a generalized volume-filling chemotaxis model with cell proliferation, *Anal. Appl.*, **15** (2017), 83–106. http://doi.org/10.1142/s0219530515500220
15. M. J. Ma, M. Y. Gao, C. P. Tong, Y. Z. Han, Chemotaxis-driven pattern formation for a reaction-diffusion-chemotaixs model with volume-filling effect, *Comput. Math. Appl.*, **72** (2016), 1320–1340. http://doi.org/10.1016/j.camwa.2016.06.039
16. Y. Z. Han, Z. F. Li, J. C. Tao, M. J. Ma, Pattern formation for a volume-filling chemotaxis model with logistic growth, *J. Math. Anal. Appl.*, **418** (2017), 885–907. http://doi.org/10.1016/j.jmaa.2016.11.040
17. M. J. Ma, M. Y. Gao, R. Carretero-Gonzalez, Pattern formation for a two-dimensional reaction-diffusion model with chemotaxis, *J. Math. Anal. Appl.*, **475** (2019), 1883–1909. http://doi.org/10.1016/j.jmaa.2019.03.060
18. S. Lynch, *Dynamical systems with applications using Maple^{TM}*, Boston, MA: Birkhäuser, 2010. https://doi.org/10.1007/978-0-8176-4605-9

A. Appendix I. The single unstable mode case

This appendix aims to give the parts omitted in the derivation of the Stuart-Landau equation and spatiotemporal pattern from the previous sections. According to the derivation of the F, G (4.7) in Section 4, we obtain the expressions of H and P as follows:

$$\begin{cases} H_1 = \frac{\partial U_3}{\partial T_1} + \frac{\partial U_2}{\partial T_2} + \frac{\partial U_1}{\partial T_3} + \frac{\mu((U_2^2+2U_1U_3)(2K-\theta)+3U_2U_1^2)}{K} \\ \quad +\chi_a(1-2K)\nabla(U_1\nabla V_3 - 2U_2U_1\nabla V_1 + U_2\nabla V_2 + U_3\nabla V_1 - U_1^2\nabla V_2) \\ \quad +\chi_1\nabla((1-2K)(U_1\nabla V_2 + U_2\nabla V_1) + (1-K)K\nabla V_3 - U_1^2\nabla V_1) \\ \quad +\chi_2\nabla((1-2K)U_1\nabla V_1 + (1-K)K\nabla V_2) + \chi_3(K-K^2)\nabla^2 V_1, \\ H_2 = \frac{\partial V_3}{\partial T_1} + \frac{\partial V_2}{\partial T_2} + \frac{\partial V_1}{\partial T_3}. \end{cases} \tag{A.1}$$

$$\begin{cases} P_1 = \frac{\partial U_4}{\partial T_1} + \frac{\partial U_3}{\partial T_2} + \frac{\partial U_2}{\partial T_3} + \frac{\partial U_1}{\partial T_4} + \frac{\mu(2(U_2U_3+U_1U_4)(2K-\theta)+3U_1(U_2^2+U_1U_3))}{K} \\ \quad +\chi_1\nabla((K-K^2)\nabla V_4 + (1-2K)(U_1\nabla V_3 + U_2\nabla V_2 + U_3\nabla V_1) - U_1^2\nabla V_2 - 2U_2U_1\nabla V_1) \\ \quad +\chi_2\nabla((K-K^2)\nabla V_3 + (1-2K)(U_1\nabla V_2 + U_2\nabla V_1) - U_1^2\nabla V_1) \\ \quad +\chi_3\nabla((K-K^2)\nabla V_2 + (1-2K)U_1\nabla V_1) + (K-K^2)\chi_4\nabla\nabla V_1 \\ \quad +\chi_a\nabla((1-2K)(U_1\nabla V_4 + U_2\nabla V_3 + U_3\nabla V_2 + U_4\nabla V_1) \\ \quad -U_1^2\nabla V_3 - 2U_2U_1\nabla V_2 - (U_2^2 - 2U_1U_3)\nabla V_1), \\ P_2 = \frac{\partial V_4}{\partial T_1} + \frac{\partial V_3}{\partial T_2} + \frac{\partial V_2}{\partial T_3} + \frac{\partial V_1}{\partial T_4}. \end{cases} \tag{A.2}$$

According to the quintic Stuart-Landau equation (4.12), we can display the solutions of Eq (4.6) as follows:

$$W_3 = (A\begin{pmatrix} a_{31} \\ b_{31} \end{pmatrix} + A^3\begin{pmatrix} a_{32} \\ b_{32} \end{pmatrix})\cos(k_a x) + A^3\begin{pmatrix} a_{33} \\ b_{33} \end{pmatrix}\cos(3k_a x). \tag{A.3}$$

By substituting $W_1,\ W_2$, and W_3 into (4.6), and comparing the coefficients on both sides, the coefficient of the equation is obtained and solved as follows:

$$\begin{aligned}
a_{31} &= \frac{(1-K)K\chi_2 k_a^2\left(d_2k_a^2+\beta\right)}{\left(d_2k_a^2+\beta\right)\left(d_1k_a^2+\mu(K-\theta)\right)+\alpha(K-1)Kk_a^2\chi_a},\\
b_{31} &= \frac{\alpha(1-K)K\chi_2 k_a^2}{\left(d_2k_a^2+\beta\right)\left(d_1k_a^2+\mu(K-\theta)\right)+\alpha(K-1)Kk_a^2\chi_a},\\
a_{32} &= -\frac{\left(d_2k_a^2+\beta\right)\left(Kk_a^2\chi_a\left(4(2K-1)MV_{21}+2(2K-1)(2U_{21}-U_{22})+M^2\right)+\mu M\left(4(2U_{21}+U_{22})(2K-\theta)+3M^2\right)\right)}{4K\left(\left(d_2k_a^2+\beta\right)\left(d_1k_a^2+\mu(K-\theta)\right)+\alpha(K-1)Kk_a^2\chi_a\right)},\\
b_{32} &= -\frac{\alpha\left(Kk_a^2\chi_a\left(4(2K-1)MV_{21}+2(2K-1)(2U_{21}-U_{22})+M^2\right)+\mu M\left(4(2U_{21}+U_{22})(2K-\theta)+3M^2\right)\right)}{4K\left(\left(d_2k_a^2+\beta\right)\left(d_1k_a^2+\mu(K-\theta)\right)+\alpha(K-1)Kk_a^2\chi_a\right)},\\
a_{33} &= -\frac{\left(9d_2k_a^2+\beta\right)\left(3Kk_a^2\chi_a\left(8KMV_{21}+4KU_{22}+M^2-4MV_{21}-2U_{22}\right)+\mu M\left(8KU_{22}+M^2-4\theta U_{22}\right)\right)}{4K\left(\left(9d_2k_a^2+\beta\right)\left(9d_1k_a^2+\mu(K-\theta)\right)+9\alpha(K-1)Kk_a^2\chi_a\right)},\\
b_{33} &= -\frac{\alpha\left(3Kk_a^2\chi_a\left(8KMV_{21}+4KU_{22}+M^2-4MV_{21}-2U_{22}\right)+\mu M\left(8KU_{22}+M^2-4\theta U_{22}\right)\right)}{4K\left(\left(9d_2k_a^2+\beta\right)\left(9d_1k_a^2+\mu(K-\theta)\right)+9\alpha(K-1)Kk_a^2\chi_a\right)}.
\end{aligned} \tag{A.4}$$

Combining $W_1,\ W_2,\ W_3$, (4.12), and (4.6), taking $\chi_1 = 0$ and $\frac{\partial W_1}{\partial T_1} = 0$, we have

$$\begin{aligned}
H_1 &= (2a_{21} + 2a_{22}\cos(2k_a x))A\frac{\partial A}{\partial T_2} + \frac{\partial A}{\partial T_3}M\cos(k_a x) + A(K^2-K)\chi_3 k_a^2\cos(k_a x)\\
&\quad + \frac{A^4H_{13}\cos(4k_a x)}{K} + \frac{(A^4H_{15}+A^2H_{14})\cos(2k_a x)}{K} + \frac{A^4H_{12}}{K} + \frac{A^2H_{11}}{K},\\
H_2 &= (2b_{21} + 2b_{22}\cos(2k_a x))A\frac{\partial A}{\partial T_2} + \frac{\partial A}{\partial T_3}\cos(k_a x),
\end{aligned} \tag{A.5}$$

where

$$\begin{aligned}
H_{11} &= M(2K-\theta)\mu a_{31},\\
H_{12} &= \tfrac{1}{4}\mu\left(a_{32}(8KM-4\theta M) + U_{22}\left(U_{22}(4K-2\theta)+3M^2\right) + U_{21}^2(8K-4\theta) + 6M^2U_{21}\right),\\
H_{13} &= 2KMk_a^2\chi_a\left(b_{33}(6K-3)+MV_{21}\right) + \tfrac{1}{4}U_{22}\left(8Kk_a^2\chi_a\left((4K-2)V_{21}+M\right)+3\mu M^2\right)\\
&\quad + a_{33}\left(2K(2K-1)k_a^2\chi_a + \mu M(2K-\theta)\right) + \mu U_{22}^2\left(K-\tfrac{\theta}{2}\right),\\
H_{14} &= Kk_a^2\left(b_{31}(2K-1)M\chi_a + \chi_2\left((2K-1)M + 4(K-1)KV_{21}\right)\right)\\
&\quad + a_{31}\left(K(2K-1)k_a^2\chi_a + \mu M(2K-\theta)\right),\\
H_{15} &= 2b_{32}K^2Mk_a^2\chi_a + 6b_{33}K^2Mk_a^2\chi_a - b_{32}KMk_a^2\chi_a - 3b_{33}KMk_a^2\chi_a + 8K^2U_{21}V_{21}k_a^2\chi_a\\
&\quad + 2KMU_{21}k_a^2\chi_a - 4KU_{21}V_{21}k_a^2\chi_a + 4K\mu U_{21}U_{22} + \tfrac{3}{2}\mu M^2U_{21} + \tfrac{3}{2}\mu M^2U_{22} - 2\theta\mu U_{21}U_{22}\\
&\quad + 2KM^2V_{21}k_a^2\chi_a + (K(2K-1)k_a^2\chi_a)(a_{32}-a_{33}) + \mu M(2K-\theta)(a_{32}+a_{33}).
\end{aligned}$$

According to the solvability conditions, we have $\int_0^l H\cdot w^* dx = 0, l = j\pi/k_a,\ j \in \mathbb{N}_+$, and

$$\frac{\partial A}{\partial T_3} = \frac{(A(K-K^2)k_a^2M^*\chi_3}{1+MM^*}.$$

Since the solution of the above equation cannot predict the evolution of the amplitude, we take $T_3 = 0$ and $\chi_3 = 0$.

Furthermore, the solution of Eq (4.7) can be written in the form:

$$W_4 = A^2\begin{pmatrix}a_{41}\\ b_{41}\end{pmatrix} + A^4\begin{pmatrix}a_{42}\\ b_{42}\end{pmatrix} + (A^2\begin{pmatrix}a_{43}\\ b_{43}\end{pmatrix} + A^4\begin{pmatrix}a_{44}\\ b_{44}\end{pmatrix})\cos(2k_a x) + A^4\begin{pmatrix}a_{45}\\ b_{45}\end{pmatrix}\cos(4k_a x). \tag{A.6}$$

Substituting $W_1,\ W_2,\ W_3,\ W_4$, and (4.12) into (4.7), taking $\chi_1 = \chi_3 = 0$, $T_1 = T_3 = 0$, $\frac{\partial W}{\partial T_1} = 0$, and

$\frac{\partial W}{\partial T_3} = 0$, and combining the solvability condition $\int_0^l H \cdot w^* dx = 0$, we have

$$
\begin{aligned}
a_{41} &= \frac{a_{31}M(\theta-2K)}{K(K-\theta)}, \quad b_{41} = \frac{\alpha a_{31}M(\theta-2K)}{\beta K(K-\theta)}, \quad a_{42} = \frac{4a_{32}M(\theta-2K)-2(2U_{21}^2+U_{22}^2)(2K-\theta)-3M^2(2U_{21}+U_{22})}{4K(K-\theta)},\\
b_{42} &= -\frac{\alpha(4a_{32}M(2K-\theta)+2(2U_{21}^2+U_{22}^2)(2K-\theta)+3M^2(2U_{21}+U_{22}))}{4\beta K(K-\theta)},\\
a_{43} &= -\frac{(4d_2k_a^2+\beta)(K(2K-1)k_a^2\chi_a(a_{31}+b_{31}M)+K\chi_2k_a^2((2K-1)M+4(K-1)KV_{21})+a_{31}\mu M(2K-\theta))}{K((4d_2k_a^2+\beta)(4d_1k_a^2+\mu(K-\theta))+4\alpha(K-1)Kk_a^2\chi_a)},\\
b_{43} &= -\frac{\alpha(K(2K-1)k_a^2\chi_a(a_{31}+b_{31}M)+K\chi_2k_a^2((2K-1)M+4(K-1)KV_{21})+a_{31}\mu M(2K-\theta))}{K((4d_2k_a^2+\beta)(4d_1k_a^2+\mu(K-\theta))+4\alpha(K-1)Kk_a^2\chi_a)},\\
a_{44} &= a'_{44} - \frac{\mu(4d_2k_a^2+\beta)(2(a_{32}+a_{33})M(2K-\theta)+4U_{21}U_{22}(2K-\theta)+3M^2(U_{21}+U_{22}))}{2K((4d_2k_a^2+\beta)(4d_1k_a^2+\mu(K-\theta))+4\alpha(K-1)Kk_a^2\chi_a)},\\
b_{44} &= b'_{44} - \frac{\alpha\mu(2(a_{32}+a_{33})M(2K-\theta)+4U_{21}U_{22}(2K-\theta)+3M^2(U_{21}+U_{22}))}{2K((4d_2k_a^2+\beta)(4d_1k_a^2+\mu(K-\theta))+4\alpha(K-1)Kk_a^2\chi_a)},\\
a_{45} &= a'_{45} - \frac{\mu(16d_2k_a^2+\beta)(a_{33}(8KM-4\theta M)+U_{22}(U_{22}(4K-2\theta)+3M^2))}{4K((16d_2k_a^2+\beta)(16d_1k_a^2+\mu(K-\theta))+16\alpha(K-1)Kk_a^2\chi_a)},\\
b_{45} &= \frac{\alpha(8Kk_a^2\chi_a((2K-1)(a_{33}+2U_{22}V_{21})+M(b_{33}(6K-3)+U_{22})+M^2V_{21})+\mu(a_{33}(8KM-4M)+U_{22}(U_{22}(4K-2\theta)+3M^2)))}{-4K((16d_2k_a^2+\beta)(16d_1k_a^2+\mu K-\theta))-16\alpha(K-1)Kk_a^2\chi_a},\\
a'_{44} &= -\frac{2Kk_a^2\chi_a((2K-1)(a_{32}-a_{33}+4U_{21}V_{21})+M((b_{32}+3b_{33})(2K-1)+2U_{21})+2M^2V_{21})}{2K(4d_2k_a^2+\beta)(4d_1k_a^2+\mu(K-\theta))+4\alpha(K-1)Kk_a^2\chi_a},\\
b'_{44} &= -\frac{2\alpha Kk_a^2\chi_a((2K-1)(a_{32}-a_{33}+4U_{21}V_{21})+M((b_{32}+3b_{33})(2K-1)+2U_{21})+2M^2V_{21})}{2K((4d_2k_a^2+\beta)(4d_1k_a^2+\mu(K-\theta))+4\alpha(K-1)Kk_a^2\chi_a)},\\
a'_{45} &= -\frac{2k_a^2\chi_a(16d_2k_a^2+\beta)((2K-1)(a_{33}+2U_{22}V_{21})+M(b_{33}(6K-3)+U_{22})+M^2V_{21})}{(16d_2k_a^2+\beta)(16d_1k_a^2+\mu(K-\theta))+16\alpha(K-1)Kk_a^2\chi_a},
\end{aligned}
\tag{A.7}
$$

and

$$\frac{\partial A}{\partial T_4} = \tilde{\sigma}A - \tilde{L}A^3 + \tilde{Q}A^5, \tag{A.8}$$

where

$$
\begin{aligned}
\tilde{\sigma} &= \frac{(1-K)KM^*k_a^2(b_{31}\chi_2+\chi_4)-\sigma(a_{31}M^*+b_{31})}{MM^*+1},\\
\tilde{L} &= \frac{M^*(a_{31}(\mu(8U_{21}(2K-\theta)+U_{22}(8K-4\theta)+9M^2)-4KL)+4((2a_{41}+a_{44})\mu M(2K-\theta)+3a_{32}K\sigma))+4K(3b_{32}\sigma-b_{31}L)}{4(K+KMM^*)}\\
&+\frac{KM^*\chi_2k_a^2(-4b_{32}(K-K^2)+8KMV_{21}-(4-8K)U_{21}-4KU_{22}+M^2-4MV_{21}+2U_{22})}{4(K+KMM^*)}\\
&+\frac{KM^*k_a^2\chi_a(2M(a_{31}+2b_{44}(2K-1))+2(2K-1)(2a_{31}V_{21}+2a_{41}-a_{44}+2b_{31}U_{21}-b_{31}U_{22})+b_{31}M^2)}{4(K+KMM^*)},\\
\tilde{Q} &= \frac{\mu M^*(-3(3a_{32}+a_{33})M^2-2M(-2(2a_{42}+a_{43})\theta+6U_{21}^2+6U_{22}U_{21}+3U_{22}^2)+4\theta(2a_{32}U_{21}+(a_{32}+a_{33})U_{22}))}{4(K+KMM^*)}\\
&+\frac{KM^*k_a^2\chi_a((4K-2)(2(a_{32}-a_{33})V_{21}+2a_{42}-a_{43}+2b_{43}M-(b_{32}-3b_{33})U_{22})+2a_{32}M-2a_{33}M)}{4(K+KMM^*)}\\
&+\frac{KM^*k_a^2\chi_a(-4U_{21}(b_{32}(1-2K)-2MV_{21}+U_{22})+b_{32}M^2+3b_{33}M^2+4U_{21}^2+2U_{22}^2)}{4(K+KMM^*)}\\
&+\frac{4K(3L(a_{32}M^*+b_{32})-2\mu M^*((2a_{42}+a_{43})M+2a_{32}U_{21}+(a_{32}+a_{33})U_{22}))}{4(K+KMM^*)}.
\end{aligned}
\tag{A.9}
$$

Since $T_i = \varepsilon^i t$, the derivative of amplitude is given by

$$\frac{dA}{dt} = \varepsilon\frac{\partial A}{\partial T_1} + \varepsilon^2\frac{\partial A}{\partial T_2} + \varepsilon^3\frac{\partial A}{\partial T_3} + \varepsilon^4\frac{\partial A}{\partial T_4}, \tag{A.10}$$

where $T_1 = 0$ and $T_3 = 0$. So we obtain

$$\frac{dA}{dt} = \varepsilon^2(\bar{\sigma}A - \bar{L}A^3 + \bar{Q}A^5), \tag{A.11}$$

where

$$\bar{\sigma} = \sigma + \varepsilon^2\tilde{\sigma}, \bar{L} = L + \varepsilon^2\tilde{L}, \bar{Q} = \varepsilon^2\tilde{Q}.$$

Let $T = \varepsilon^2 t$, and then $dT = \varepsilon^2 dt$. So we obtain the amplitude equation (4.16).

B. Appendix II. The double unstable mode case

In this section, the derivation of double unstable mode case is given. Let k_1^2 and k_2^2 be unstable modes of model (1.2). We presume that w^* is a fundamental solution of $L^*w^* = 0$, where L^* is the adjoint operator of $\mathcal{L}(\chi_c)$.

$$w^* = (M_1^*, 1)^T \cos(k_1 x) + (M_2^*, 1)^T \cos(k_2 x) \tag{B.1}$$

where

$$M_1^* = \frac{\alpha}{d_1 k_1^2 + \mu(K - \theta)}, M_2^* = \frac{\alpha}{d_1 k_2^2 + \mu(K - \theta)}.$$

Substituting (4.21) into $F = (F_1, F_2)^T$, we have

$$\begin{aligned}
F_1 = {} & \frac{A_1^2 \cos(2k_1 x)\left(M_1\left(2k_1^2 K(2K-1)\chi_a+\mu M_1(2K-\theta)\right)\right)}{2K} + \frac{A_1^2\left(K\mu M_1^2-\frac{1}{2}\theta\mu M_1^2\right)}{K} \\
& + \frac{A_2^2 \cos(2k_2 x)\left(M_2\left(2k_2^2 K(2K-1)\chi_a+\mu M_2(2K-\theta)\right)\right)}{2K} + \frac{A_2^2\left(K\mu M_2^2-\frac{1}{2}\theta\mu M_2^2\right)}{K} \\
& + \frac{A_1 A_2 \cos(k_1 x-k_2 x)\left(k_1(k_1-k_2)\left(2K^2-K\right)M_2\chi_a+2M_1(M_2(4K\mu-2\theta\mu)-(k_1-k_2)k_2 K(2K-1)\chi_a)\right)}{2K} \\
& + \frac{A_1 A_2 \cos(k_1 x+k_2 x)(M_1(k_2(k_1+k_2)K(2K-1)\chi_a+M_2(4K\mu-2\theta\mu))+k_1(k_1+k_2)K(2K-1)M_2\chi_a)}{2K} \\
& + \frac{\partial A_1}{\partial T_1} M_1 \cos(k_1 x) + \frac{\partial A_2}{\partial T_1} M_2 \cos(k_2 x), \\
F_2 = {} & \frac{\partial A_1}{\partial T_1} \cos(k_1 x) + \frac{\partial A_2}{\partial T_1} \cos(k_2 x).
\end{aligned}$$

So we assume that Eq (4.4) has solutions as in (4.24). Substituting W_1, W_2, and (4.24) into (4.4), combining the solvability condition for (4.4), i.e., $\int_0^l F \cdot w^* dx = 0$, and setting $\chi = 0$ and $T_1 = 0$, then we obtain (4.24) and its coefficients as follows:

$$\begin{aligned}
F_{11} &= -\frac{M_1^2(2K-\theta)}{2K(K-\theta)}, \quad F_{12} = -\frac{\left(\beta+4d_2 k_1^2\right)\left(2k_1^2(2K^2-K)M_1\chi_a+\mu M_1^2(2K-\theta)\right)}{8\alpha k_1^2(K-1)K^2\chi_a+K\left(\beta+4d_2 k_1^2\right)\left(8d_1 k_1^2+2\mu(K-\theta)\right)}, \\
F_{13} &= -\frac{M_2^2(2K-\theta)}{2K(K-\theta)}, \quad F_{14} = -\frac{\left(\beta+4d_2 k_2^2\right)\left(2k_2^2(2K^2-K)M_2\chi_a+\mu M_2^2(2K-\theta)\right)}{8\alpha k_2^2(K-1)K^2\chi_a+K\left(\beta+4d_2 k_2^2\right)\left(8d_1 k_2^2+2\mu(K-\theta)\right)}, \\
F_{15} &= -\frac{\left(\beta+d_2(k_1-k_2)^2\right)\left(2\mu M_1 M_2(2K-\theta)-(k_1-k_2)\left(2K^2-K\right)\chi_a(k_2 M_1-k_1 M_2)\right)}{2\alpha(k_1-k_2)^2(K-1)K^2\chi_a+K\left(\beta+d_2(k_1-k_2)^2\right)\left(2d_1(k_1-k_2)^2+2\mu(K-\theta)\right)}, \\
F_{16} &= \frac{\left(\beta+d_2(k_1+k_2)^2\right)\left((k_1+k_2)\left(2K^2-K\right)\chi_a(k_2 M_1+k_1 M_2)+2\mu M_1 M_2(2K-\theta)\right)}{2\alpha(k_1+k_2)^2(1-K)K^2\chi_a+K\left(-\beta-d_2(k_1+k_2)^2\right)\left(2d_1(k_1+k_2)^2+2\mu(K-\theta)\right)}, \\
F_{21} &= -\frac{\alpha M_1^2(2K-\theta)}{2\beta K(K-\theta)}, \quad F_{22} = \frac{\alpha\left(2k_1^2\left(K-2K^2\right)M_1\chi_a-\mu M_1^2(2K-\theta)\right)}{8\alpha k_1^2(K-1)K^2\chi_a+K\left(\beta+4d_2 k_1^2\right)\left(8d_1 k_1^2+2\mu(K-\theta)\right)}, \\
F_{23} &= -\frac{\alpha M_2^2(2K-\theta)}{2\beta K(K-\theta)}, \quad F_{24} = \frac{\alpha\left(2k_2^2\left(K-2K^2\right)M_2\chi_a-\mu M_2^2(2K-\theta)\right)}{8\alpha k_2^2(K-1)K^2\chi_a+K\left(\beta+4d_2 k_2^2\right)\left(8d_1 k_2^2+2\mu(K-\theta)\right)}, \\
F_{25} &= \frac{\alpha((k_1-k_2)K(1-2K)\chi_a(k_1 M_2-k_2 M_1)+M_1(2\mu M_2(\theta-2K)))}{(k_1-k_2)^2\left(d_1\left(\beta+d_2(k_1-k_2)^2\right)-\alpha\left(K^2+K\right)\chi_a\right)+(K-\theta)\left(\beta\mu+d_2(k_1-k_2)^2\mu\right)} \\
F_{26} &= \frac{\alpha\left((k_1+k_2)\left(2K^2-K\right)\chi_a(k_2 M_1+k_1 M_2)+2\mu M_1 M_2(2K-\theta)\right)}{K\left(-\beta-d_2(k_1+k_2)^2\right)\left(2d_1(k_1+k_2)^2+2\mu(K-\theta)\right)-2\alpha(k_1+k_2)^2\left(K^3-K^2\right)\chi_a}.
\end{aligned} \tag{B.2}$$

By substituting W_1 and W_2 into $G = (G_1, G_2)^T$, and combining the solvability condition for (4.5), i.e., $\int_0^l F \cdot w^* dx = 0, l = 2\pi/k_i, i = 1, 2$, (4.25) is given. Since the expressions are too long, we omit it and just give the integral result, i.e., the amplitude equations of the double unstable modes (4.22). The coefficients of the equation are as follows:

$$
\begin{aligned}
\tau_1 &= -\frac{\chi_2 k_1^2 M_1^*(K-K^2)}{1+M_1M_1^*}, \tau_2 = -\frac{\chi_2 k_2^2 M_2^*(K-K^2)}{1+M_2M_2^*},\\
L_1 &= \frac{M_1^*(2k_1^2K(1-2K)\chi_a(-2F_{22}KM_1-2F_{11}+F_{12})+M_1^2\left(k_1^2K\chi_a+3\mu M_1\right)+(2F_{11}+F_{12})\mu M_1(8K-4\theta))}{16K^2\left(1+M_1M_1^*\right)},\\
L_2 &= \frac{M_2^*(2k_2^2K(1-2K)\chi_a(-2F_{22}KM_2-2F_{13}+F_{14})+M_2^2\left(k_2^2K\chi_a+3\mu M_2\right)+(2F_{13}+F_{14})\mu M_2(8K-4\theta))}{16K^2\left(1+M_2M_2^*\right)},\\
Q_1 &= \frac{M_1^*}{4K^3(1+M_1M_1^*)}(\mu((2F_{13}M_1 + F_{15}M_2 + F_{16}M_2)(4K-2\theta) + 3M_1M_2^2)\\
&\quad +\chi_a k_1 K((1-2K)(M_2(k_2(F_{25}-F_{26}) - k_1(F_{25}+F_{26})) + (F_{16}-F_{15})k_2 - 2F_{13}k_1) + k_1M_2^2)),\\
Q_2 &= \frac{M_2^*}{4K^2(1+M_2M_2^*)}(\mu((F_{15}M_1 + F_{16}M_1 + 4F_{11}M_2)(4K-2\theta) + 3M_2M_1^2)\\
&\quad +\chi_a k_2 K((1-2K)(M_1(k_1(F_{25}-F_{26}) - k_2(F_{25}+F_{26})) + (F_{16}-F_{15})k_1 - 2F_{11}k_2) + k_2M_1^2)).
\end{aligned} \tag{B.3}
$$